Free Radical Research, November 2006; 40(11): 1124–1137

informa
healthcare

ROS and protein oxidation in early stages of cytotoxic drug induced apoptosis

KAREN ENGLAND, CAROLYN O. 'DRISCOLL & THOMAS G. COTTER

Department of Biochemistry, Biosciences Institute, University College Cork, Cork, Ireland

Accepted by Professor M. Jackson

(Received 24 March 2006; in revised form 14 May 2006)

Abstract
Cytotoxic drugs induce cell death through induction of apoptosis. This can be due to activation of a number of cell death pathways. While the downstream events in drug induced cell death are well understood, the early events are less clear. We therefore used a proteomic approach to investigate the early events in apoptosis induced by a variety of drugs in HL60 cells. Using 2D-gel electrophoresis, we were able to identify a number of protein changes that were conserved between different drug treatments. Identification of post-translational modifications (PTM) responsible for these proteome changes revealed an increase in protein oxidation in drug treated cells, as well as changes in protein phosphorylation. We demonstrate an accumulation of oxidised proteins within the ER, which lead to ER stress and calcium release and may result in the induction of apoptosis. This study demonstrates the importance of ROS mediated protein modifications in the induction of the early stages of apoptosis in response to chemotherapeutic drug treatment.

Keywords: *Post-translational modifications, proteomics, apoptosis, carbonylation, ER stress, leukaemia*

Abbreviations: *ER, endoplasmic reticulum; H_2DCFDA, 2′7′-dichlorodihydrofluorescein diacetate (2′7′-dichlorofluorescin diacetate); NAC, N-acetyl-L-cysteine; PDI, protein disulphide isomerase; PTM, post-translational modification; ROS, reactive oxygen species; TBS, Tris-buffered saline; UPR, unfolded protein response; zVAD-fmk, Z-Val-Ala-Asp.fluoromethyketone*

Introduction

The aim of chemotherapy is to preferentially kill tumour cells, whilst leaving normal cells alive [1]. Chemotherapeutic drugs are derived from a number of different drug families, such as alkylating agents, mitotic inhibitors, nitrosureas, antimetabolites, and antitumour antibiotics. These drugs predominantly induce cell death through apoptosis, or programmed cell death, rather than necrosis. Of the drugs employed in this study, both doxorubicin (Doxo) and mitoxantrone (Mtx) are anticancer antibiotics, whereas VP16 (etoposide) is an epipodophylotoxin and classified as a mitotic inhibitor. All of these drugs have been shown to induce cell death through apoptosis. Apoptotic cell death typically, although not always, is mediated through the activation of a group of enzymes known as caspases. Other cellular characteristics of apoptosis include mitochondrial depolarisation, DNA fragmentation and the appearance of phosphatidyl serine on the outside of the cellular membrane [2]. These late apoptotic events are well characterised, but the upstream pathways leading to caspase activation and cell death are more diverse and variable. Apart from a few defined pathways of caspase activation, such as caspase 8 activation by Fas and TNF receptors, upstream events are not well understood. In this paper, we have used proteomics to

Correspondence: T. Cotter, Department of Biochemistry, Biosciences Institute, University College Cork, Cork, Ireland. Tel: 353 21 4901321. Fax: 353 21 4901382. E-mail: t.cotter@ucc.ie

ISSN 1071-5762 print/ISSN 1029-2470 online © 2006 Informa UK Ltd.
DOI: 10.1080/10715760600838209

study events upstream of caspase activation in response to a number of chemotherapeutic agents. Understanding the exact mechanisms behind the induction of cell death in response to these agents is important in understanding toxicity and side effects, for example, Doxo mediated cardiotoxicity is mediated not through its topoisomerase II inhibition, but rather through the production of reactive oxygen species (ROS) [3].

It is impossible to predict the mechanism of drug mediated caspase activation as cytotoxic drugs mediate their effects through a number of different mechanisms, not limited to their "mode of action". For example, it has been shown that many cytotoxic drugs can induce ROS, or can induce apoptosis through the direct modulation of signalling proteins, such as the induction of stress activated cell signalling pathways [2]. Reports of drug "mode of action" are often conflicting; although there are some reports that VP16, a topisomerase II inhibitor can also mediate cell death through the induction of ROS, whilst, other work suggests that VP16 induced cell death is independent of ROS as it cannot be prevented by antioxidant treatment [4–6]. As well as topisomerase inhibition Doxo has been shown to produce ROS [7–9], which are at least in part responsible for its induction of apoptosis, as well as the induction of p38 MAP kinase (p38 MAPK), a stress activated kinase [10]. Mtx, a Doxo analogue with reduced cardiotoxicity can also induce activation of p38 MAPK [11]. ROS generated by cytotoxic drugs can result in DNA damage and strand breaks, as well as protein oxidation. Such oxidation events further increase cell stress, which may contribute to the induction of cell death.

The three cytotoxic drugs employed in this study are widely used in the clinical environment in the treatment of a number of cancers. All three drugs have been reported to exert their cellular effects through a variety of mechanisms including DNA damage and topoisomerase II inhibition. The initial effects of these drugs upon the cell are key for the induction of apoptosis. We therefore decided to investigate the early effects of cytotoxic drug treatment, in particular, early protein changes which may be responsible for induction of cell death signalling. Many signalling pathways depend on changes in a variety of post-translational protein modifications (PTM), such as phosphorylation, oxidation, s-nitrosylation and ADP ribosylation. In order to identify these early events, we use a proteomic approach to investigate proteomic changes in cells undergoing relatively rapid apoptosis, (50% after 4 h of treatment). HL60 cells are a human heamatopoietic cell line, which readily undergo apoptosis in response to a number of stimuli making them ideal for this study. This experimental design, with its short exposure time, will increase the number of cells exhibiting early changes in protein states allowing more accurate determination of the PTM involved. Under these conditions, it is likely that alterations in gene expression will not have a role to play, instead it is likely that protein modifications will be important indicators of the signalling pathways involved in cell death.

Proteomic analysis will enable us to look for number of PTM of proteins. A number of PTMs have been associated with cell death pathways. Phosphorylation is a key PTM for many signalling pathways. Protein kinases and phosphatases play vital role in cell survival pathways and more recently, phosphorylation of apoptotic regulators, such as Bcl-2 family members, have demonstrated their importance in cell death pathways [12]. There are a number of other PTMs which are been implicated in cell death in a variety of systems; these include ADP ribosylation [13–15], protein s-nitrosylation [16–18] and protein oxidation [19,20]. Caspases themselves can undergo s-nitrosylation of their active site which results in their inactivation [17,21]. The finding that many drugs induce a rapid increase in cellular ROS is of interest as ROS can induce apoptosis through a variety of mechanisms; including direct modification of proteins, as well as lipids and DNA. Modification of proteins by ROS generally inactivates them [4,22]. Although ROS mediated protein inactivation is non-specific and both pro and anti-apoptotic proteins may be targeted; so pro-apoptotic proteins such as caspases can be inactivated as well as survival proteins such as Ras. This makes it difficult to predict the effect of ROS in cytotoxic drug mediated cell death.

This work describes the use of proteomics to study early events in chemotherapeutic drug induced apoptosis. Identification of PTM will broaden out understanding of how such drugs induce cell death. A better understanding of the mechanism of drug induced cell death is essential in order to reduce side effects or to increase efficiency of these drugs.

Materials and methods

Chemicals and antibodies

All chemicals were from Sigma (Dublin, Ireland) unless otherwise indicated. The anti-caspase 3 antibody (Cell Signalling, Beverley, MA, USA) was used at 1/1000. The anti-DNP antibody (Dako, UK) was used at 1/5000. The phospho-eIF 2α (Cell Signalling Technology, Beverley, MA, USA) was used at 1/1000. Triose phosphate isomerase and phosphoglycerate mutase (both from Accurate Chemical and Scientific, NY, USA), Grp78 (Santa Cruz, sc13968), Hsp 70 (AB5439 AbCam). The anti-actin antibody (Sigma) used for equal loading controls was used at 1/5000. HRP conjugated secondary antibodies were from Sigma.

Cell culture and cytotoxic drug treatment

HL60 cells were maintained in RPMI 1640 supplemented with 10% foetal calf serum, 1% penicillin–streptomycin and 2 mM L-glutamine (Gibco Brl, Paisley, UK). Cells were grown at 37°C in a humidified 5% CO_2 atmosphere. VP16, Mtx and Doxo were prepared in DMSO. For induction of apoptosis, 5×10^5 cells/ml were incubated for the appropriate time and drug at 37°C. Treatment with *N*-acetyl cysteine (Calbiochem, Nottingham, UK) and zVAD (Enzyme System Products, CA, USA) was for 30 min prior to the addition of VP16.

Detection of apoptosis

Cell death was measured by incorporation of 50 μg/ml propidium iodide on a FACScan (Becton and Dickinson, UK) using CellQuest software. Apoptosis was confirmed by morphological analysis of stained cytospin preparations. Rapi-diff (Diachem International Ltd., Lancashire, UK) stained centrifuged cell preparations were examined for the morphological characteristics of apoptosis. Apoptosis was quantified by counting three independent microscopic fields with at least 100 cells per field.

FACS analysis of ROS generation

HL60 cells at 5×10^5 were treated with VP16, Mtx or Doxo for the times indicated and 100 μM 2′,7′-dichlorodihydrofluorescein diacetate (H_2DCFDA) (2′,7′-dichlorofluorescin diacetate) (Molecular Probes, Leiden, The Netherlands) was added 30 min before analysis on a FACScan (Becton and Dickinson, Oxford, UK) with excitation and emission spectra set at 488 and 530 nm using CellQuest software. H_2O_2 was visualised by the increase in mean fluorescence.

Spectrophotometric detection of protein carbonylation

Protein carbonylation was determined as described by Levine et al. (1990) [23]. Basically protein was extracted into 100 μl of 40 mM Tris. To this was added 20 μl of 10 mM 2,4-dinitrophenyl hydrazine (DNPH) for 30 min at 18°C. Protein was precipitated by the addition of an equal volume of ice cold 10% TCA and incubation on ice for 30 min. Protein was pelleted by centrifugation at 15,000*g* for 5 min and the protein pellet resuspended in 6 M guanidine with 2 mM potassium phosphate and absorbance measured at 360 nm. Un-derivitised samples were used as controls. Protein determination was carried out using the Bradford based BioRad protein determination assay (BioRad Cat No 500-0001) according to manufacturers instructions. Protein carbonylation was calculated as μM DNPH per g of protein.

2D-gel electrophoresis

HL60 cells (10 ml at 5×10^5 cells/ml) were centrifuged at 1000*g* for 5 min, washed in 0.25 M sucrose before being washed and resuspended in 40 mM Tris containing phosphatase and protease inhibitors (10 μg/ul aprotinin, 10 μg/ml leupeptin, 2 mM AEBSF, 50 mM NaF, 5 mM Na pyrophosphate, 10μM Na orthovanadate). Samples were sonicated and centrifuged at 15,000*g* for 15 min. Protein was quantified using the BioRad protein determination assay and 20 μg was suspended in 1 M thiourea, 8 M urea, 4% CHAPS, 2 mM tributylphosphine with the addition of the appropriate carrier ampholytes, (pH 3–10, Amersham Bioscicences, Chalfont St Giles, Bucks., UK). Isoelectric focusing was carried out on an IPGPhor (Amersham Biosciences) using 7 cm pH 3–10 Immoboline Dry Strip Gels (Amersham Biosciences) using a gradient from 500 to 5000 V to give a total of 8750 Vh. After isoelectric focusing gels, strips were incubated for 14 min in 50 mM Tris pH 8.8, 6 M urea, 30% (v/v) glycerol, 2% SDS, 2% DTT, followed by 4 min in 50 mM Tris pH 8.8, 6 M Urea, 30% (v/v) glycerol, 2% SDS, 2.5% iodoacetamide, prior to resolving by SDS-PAGE on 10% acrylamide gel. For detection of carbonylated proteins, gel strips were incubated in 10 mM DNPH in 2 M HCl for 20 min after isoelectric focussing but prior to resolving by SDS-PAGE.

Gel staining and analysis

For analysis, gels were stained with Colloidal Blue Coomassie (Sigma) according to manufacturers instructions. Silver stained gels were fixed in 40% EtOH, 10% HAC, 50% H_2O, for 1 hour and then in 90% H_2O, 5% EtOH, 5% HAC overnight. Gels were soaked in 1% gluteraldehyde, 0.5 M sodium acetate for 30 min, washed three times in H_2O, incubated in ammonical silver for 30 min before washing in water and developing in 0.01% citric acid/0.1% formaldehyde and stopped in 5% Tris/2% acetic acid. Gels were scanned on an Epson Expression 1600 pro scanner and analysed using Phoretix 2D-gel analysis programme (Non Linear Dynamics, Newcastle, UK). At least four duplicate gels were matched and analysed for each time point. To compare, spot intensity values were normalised to regions of gel that did not contain any detectable spots. Analysis of silver stained gels detected an average of 1436 spots (SD = 278) and for coomassie stained gels, an average of 454 spots were detected (SD = 42).

For MALDI-TOF MS analysis, spots were homogenised in 25 mM ammonium bicarobonate/50% ACN, dried in a vacuum centrifuge and resuspended in 0.05 μg/μl Trypsin (Roche, Basel, Switzerland) in 25 mM ammonium bicarbonate/5 mM CaCl. Spots were digested at 37°C overnight. Peptides were eluted

in 50% ACN/5%TFA and concentrated in a vacuum centrifuge. Salt was removed using ZipTips (Millipore, MA, USA).

MALDI-TOF mass spectrometry

Mass spectrometry was carried out using a Voyager-DePro Biospectrometry workstation and Voyager Software (Applied Biosystems, Warrington, UK). MALDI-TOF mass spectrometry was performed in reflector mode and a multipoint calibration performed. Minimal machine resolution was 7000. Spectra obtained were matched through Protein Prospector MS-Fit (http://www.prospector.ucsf.edu) and MASCOT (http://www.matrixscince.com). For database searching, all species were searched, with a mass tolerance of ± 0.2 Da. For protein prospector, highest ranking matches with MOWSE scores $>1 \times 10^3$, for MASCOT significant protein matches ($P < 0.05$) were considered further. Highest ranking protein matches were confirmed through repetition (in all cases, identical protein identities were obtained from a minimum of three independent protein extractions) and through analysis of mass spectra obtained from proteins digested with Endoproteinase Glu C (Roche) as an alternative to trypsin.

Western blotting

For conventional Western blotting, 50 μg of protein was loaded per sample. After SDS-PAGE on the BioRad Mini-Protean II system, protein was transferred to nitrocellulose membrane (Schleicher and Schuell, Dassel, Germany). Proteins were detected using ECL (Amersham Biosciences).

Immunoprecipitation

Equal amounts of protein (500 μg) were resuspended in immunoprecipitation buffer (50 mM Tris–HCl, 0.5 mM EDTA, 2 mM EGTA, pH 7.5, 0.5% NP40, 10 μg/ul aprotinin, 10 μg/ml leupeptin, 2 mM AEBSF, 50 mM NaF, 5 mM Na pyrophosphate, 10μM Na orthovanadate), pre-cleared for 2 h by the addition of protein A sepharose beads and then incubated overnight with 10 μg of antibody, followed by addition of protein A sepharose. The pellet was washed twice with IP buffer before resuspending in 2D-gel lysis buffer.

For DNPH modified immunoprecipitations, the procedure was carried out as detailed above with the following modifications. After the final incubation with protein A sepharose, the protein pellet was washed three times in immunoprecipitation buffer before being resuspended in 10 mM DNPH in 2 M HCl for 20 min. The pellet was washed three times in PBS before resuspension in SDS-PAGE sample buffer and resolution by SDS-PAGE.

Measurement of intracellular free calcium

Cytosolic-free Ca^{2+} was determined with the Ca^{2+} sensitive cell permeable dye, Calcium green (Molecular Probes). Cells at 5×10^5 were washed and resuspended in PBS and loaded with Calcium green for 30 min at room temperature. Cells were then washed twice and resuspended in PBS. After 15 min, fluorescence was recorded using a Becton and Dickenson FacsScan flow cytometer on Fl-1 channel. For ER Ca^{2+} release studies, cells were further treated with 2.5μM thapsigargin and fluorescence was recorded immediately.

All data shown is representative of at least three independent experiments.

Results

Drug induced cell death

Using HL60 cells as our model system, we used propidium iodide incorporation and flow cytometry to determine the concentration of drug required to circa 50% death after 4 h of drug treatment with VP16, Mtx and Doxo. HL60 cells were treated with VP16 at 5 μg/ml and with Mtx or Doxo at 10 μg/ml, for time points up to and including 4 h (Figure 1A). After 4 h of treatment, there was approximately 50% cell death. Western blot analysis showed that pro-caspase 3 was cleaved to its active form after 3 h of VP16, Mtx, or Doxo treatment, Figure 1B, there was no evidence of caspase activation prior to 3 h. This indicates that cell death is mediated through the classical apoptotic pathway, which involves activation of this executor caspase. Pre-treatment with the caspase inhibitor zVAD significantly reduces, but does not abrogate, VP16, Mtx and Doxo induced apoptosis in HL60 cells, Figure 1C, demonstrating the importance of the caspase-dependant pathway in the induction of cell death. As the aim of our study was to identify early protein changes in response to drug treatment, we chose time points prior to caspase cleavage, at 3 h, for further study. 2D-gel electrophoresis was used to identify changes in protein expression in cytotoxic drug treated cells. 20 protein spots were found to be consistently altered upon treatment with VP16, Mtx or Doxo (data not shown). These protein spots of interest were excised from coomassie stained gels, trypsin digested and analysed by MALDI-TOF MS. The results of peptide fingerprinting are shown in Table I. After protein identification, we performed a number of experiments to determine the nature of the protein changes seen. We were unable to identify any protein spots which were unique to either treated or untreated cells, either by gel image analysis or through S^{35} methionine incorporation data, suggesting that there was no significant change in protein expression or degradation during the 3 h drug treatment. As protein phosphorylation is one of the most common

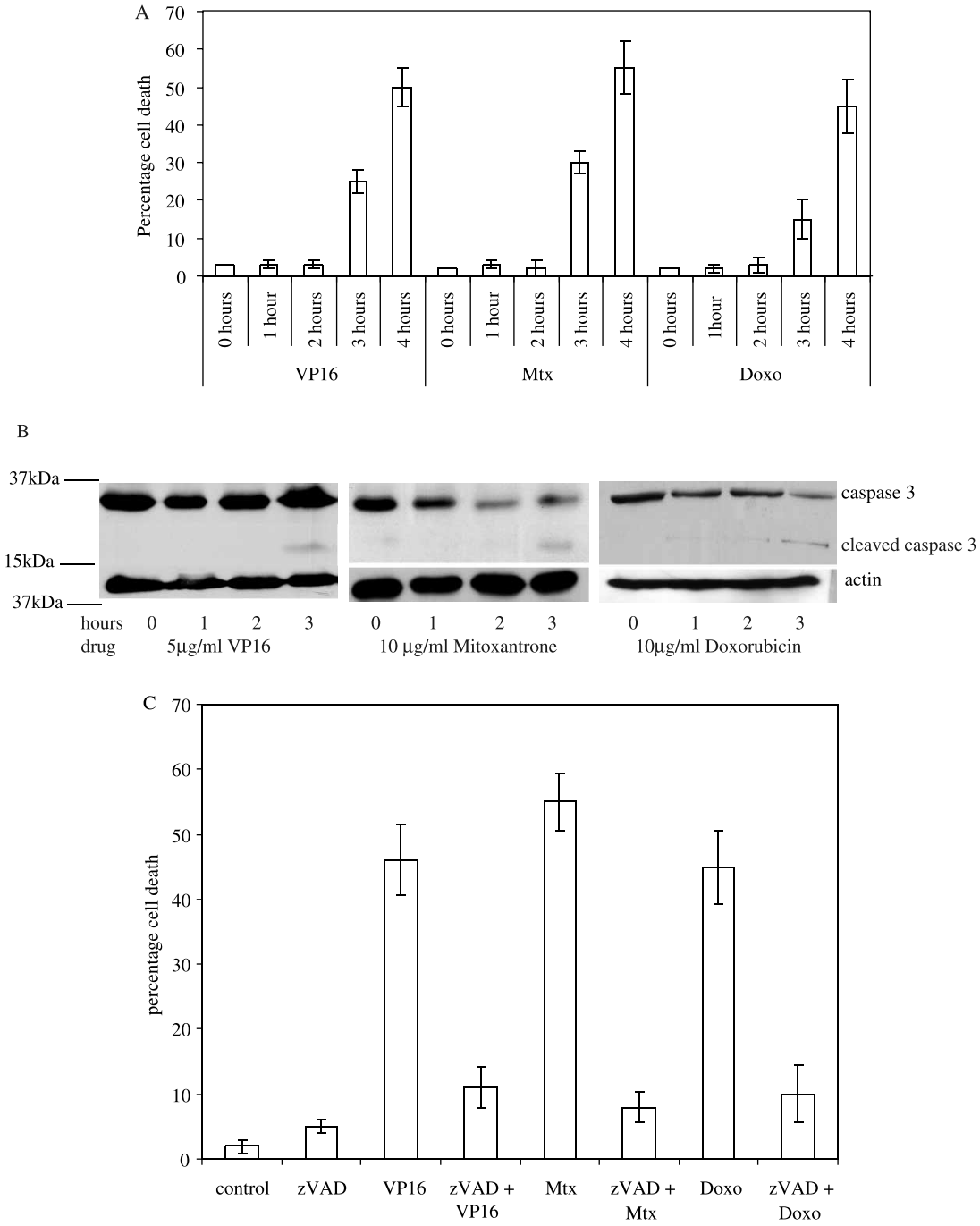

Figure 1. Induction of caspase dependant apoptosis by VP16, Mtx and Doxo in HL60 cells. A. Time course of drug induced cell death. Cells were treated with 5 µg/ml VP16, 10 µg/ml Mtx or 10 µg/ml Doxo and percentage of death was recorded using propidium iodide and flow cytometry. B. Western blot analysis showing cleavage of pro-caspase 3 to the active form of caspase 3 occurs after 3 h of VP16, Mtx and Doxo treatment. C. VP16, Mtx and Doxo induced cell death is caspase dependant. HL60 cells were pre-incubated with 100 µM of the caspase inhibitor zVAD. Cell death was analysed using propidium iodide and flow cytometry.

PTM with relevance to cell signalling, we expected to see several changes in protein phosphorylation. However, this was not the case. Using P^{32} orthophosphate incorporation to look at changes in protein phosphorylation during VP16 treatment, we saw only a few protein spots changing upon VP16 (data not shown). These include protein disulphide isomerase, an ER resident protein important in protein disulphide bond formation [24–26]. We also identified one of the phosphorylated spots as 40s ribosomal protein, a member of the ribosomal protein family, which is associated with drug resistance. p38 MAPK was also shown to undergo cytotoxic drug treatment dependant phosphorylation. p38 MAPK is commonly phosphorylated in response to cell stress situations and has been implicated in both the induction of and prevention of cell death [27–29]. p38 MAPK can phosphorylate and thus inactivate caspase 3 [30] and

Table I. Identification of proteins of interest.

Spot no.	Protein name	MW (kDa)	pI	Sample source	No. of peptides	Sequence coverage (%)
1	90 kDa Heat shock protein	85	5.0	DNP IP/2D-gel/Glu C	13	22
2	Grp78	72	5.0	DNP IP/2D-gel/Glu C	8	17
3	70 kDa Heat shock protein	75	6.3	DNP IP/2D-gel/Glu C	15	28
4	ATP synthase Beta chain	56	5.3	2D-gel/Glu C	10	29
5	Calreticulin	48	4.3	DNP IP/2D-gel	6	18
6	Tubulin	50	5.0	DNP IP/2D-gel	10	23
7	Protein disulphide isomerase	57	6.0	P^{32} incorporation DNP IP/2D-gel	6	18
8	Glycogen phosphorylase	97	6.7	2D-gel	7	20
9	Alpha enolase	47	7.0	DNP IP/2D-gel/Glu C	9	22
10	40s Ribosomal protein	33	4.8	P^{32} incorporation/2D-gel/Glu C	6	23
11	Inorganic pyrophosphatase	33	5.5	2D-gel	6	18
12	Fructose bisphosphate aldolase	39	8.4	DNP IP/2D-gel	7	30
13	Tropomyosin	32	4.7	2D-gel/Glu C	6	21
14	Endoplamic reticulum protein ERP29	29	6.8	DNP IP/2D-gel/Glu C	5	19
15	Phosphoglycerate mutase	29	6.8	DNP IP/2D-gel/Glu C	6	23
16 &17	Triose phosphate isomerase	27	6.5	DNP IP/2D-gel	10	28
18	Prohibitin	30	5.6	2D-gel/Glu C	7	22
19	RHO GDP dissociation inhibitor 2	23	5.1	2D-gel	6	25
20	Glutathione S-transferase	23	5.4	2D-gel	7	22
21	p38 MAPK	42	5.7	PhosphoTyr IP/2D-gel	8	26

Spots of interest were excised from coomassie-stained gels and analysed using MALDI-TOF MS peptide mass fingerprinting. Protein identifications were carried out using Protein Prospector MS-Fit (http://www.prospector.ucsf.edu) and MASCOT (http://www.matrixscience.com). For database searching, all species were searched, with a mass tolerance of ± 0.2 Da. Proteins are listed along with their MW in kDa, pI, mode of identification, number of peptide matched using MS-Fit, sequence coverage. All matches shown were highest ranking matches in Protein Prospector, (with MOWSE scores $>1 \times 10^3$) and significant in MASCOT ($P < 0.05$). Where indicated protein identification was carried out using peptide mass fingerprinting of spots to be DNP immunoreactive from 2D-gels, from protein immunoprecipitated using DNP, or from samples shown to change in phosphorylation state in response to cytotoxic drug treatment. Where indicated the sample identification was confirmed using GluC digestion as an alternative to trypsin.

p53 [31]. p38 MAPK phosphorylation is often linked to cell stress, such as that induced by an increase in intracellular ROS, we therefore looked for evidence for ROS in our cytotoxic drug treated cells, and any evidence for ROS mediated protein modifications.

ROS and cytotoxic drug treatment

It has reported by us and others, that VP16 and other drugs can induce intracellular ROS production [19,20,32]. In order to confirm the production of ROS in HL60 cells in response to drug treatment, we used the fluorescent probe H_2DCFHDA. Interestingly, all three drugs resulted in increased ROS levels within HL60 cell after 15 min (Figure 2A and B). If drug treatment induces ROS production, it is reasonable to predict that protein oxidation will occur within the cells. We therefore looked for evidence of protein oxidation in VP16, Mtx and Doxo treated cells, using protein carbonylation as a marker. Protein carbonylation can be determined spectrophotometrically by DNPH incorporation. This assay showed that treatment of HL60 cells with all three drugs resulted in an increase in protein carbonylation after 1 h (Figure 2C), importantly this can be prevented by pre-treatment with the antioxidant NAC. Pre-treatment of HL60 cells with the NAC also significantly reduces VP16 induced cell death, demonstrating the importance of increased ROS in VP16 mediated cell toxicity (Figure 2D). 2D-gel Western blotting of DNPH modified proteins (Oxyblots), showed patterns of proteins which have undergone carbonylation in VP16, Mtx and Doxo treated HL60 cells. Interestingly, we found that similar proteins underwent carbonylation in response to treatment with all three drugs (Figure 2E). By matching to master gels and immunoprecipitation of carbonylated proteins, as described previously [20], a number of the putative carbonylated proteins were identified, Table I. These include several glycolytic and ER resident proteins, Table II. We have previously reported the ER to be especially sensitive to protein carbonylation in response to peroxide treatment of cells [20] and that carbonylation of a number of glycolytic proteins occurs in response to VP16 treatment of HL60 cells [19]. We

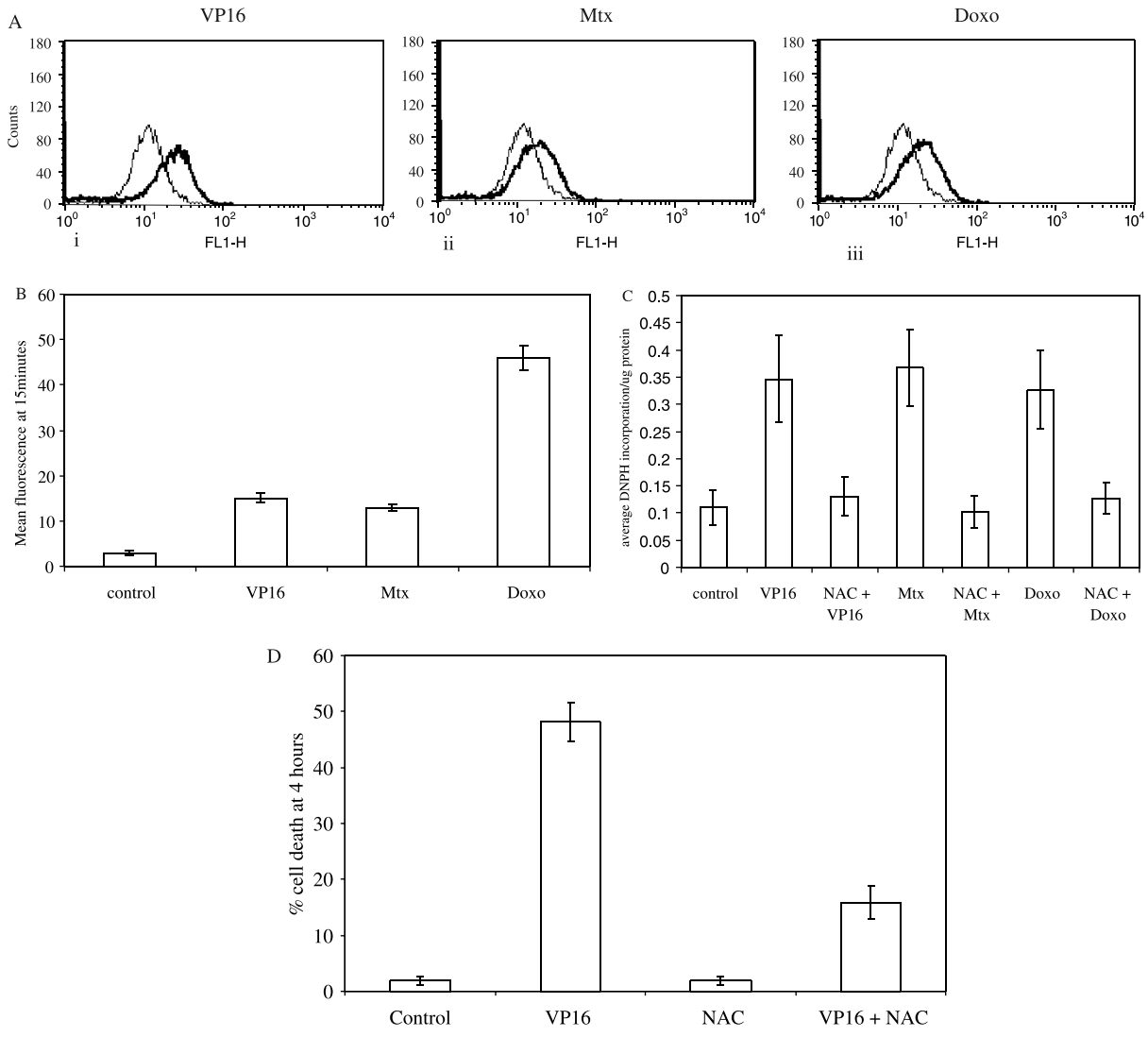

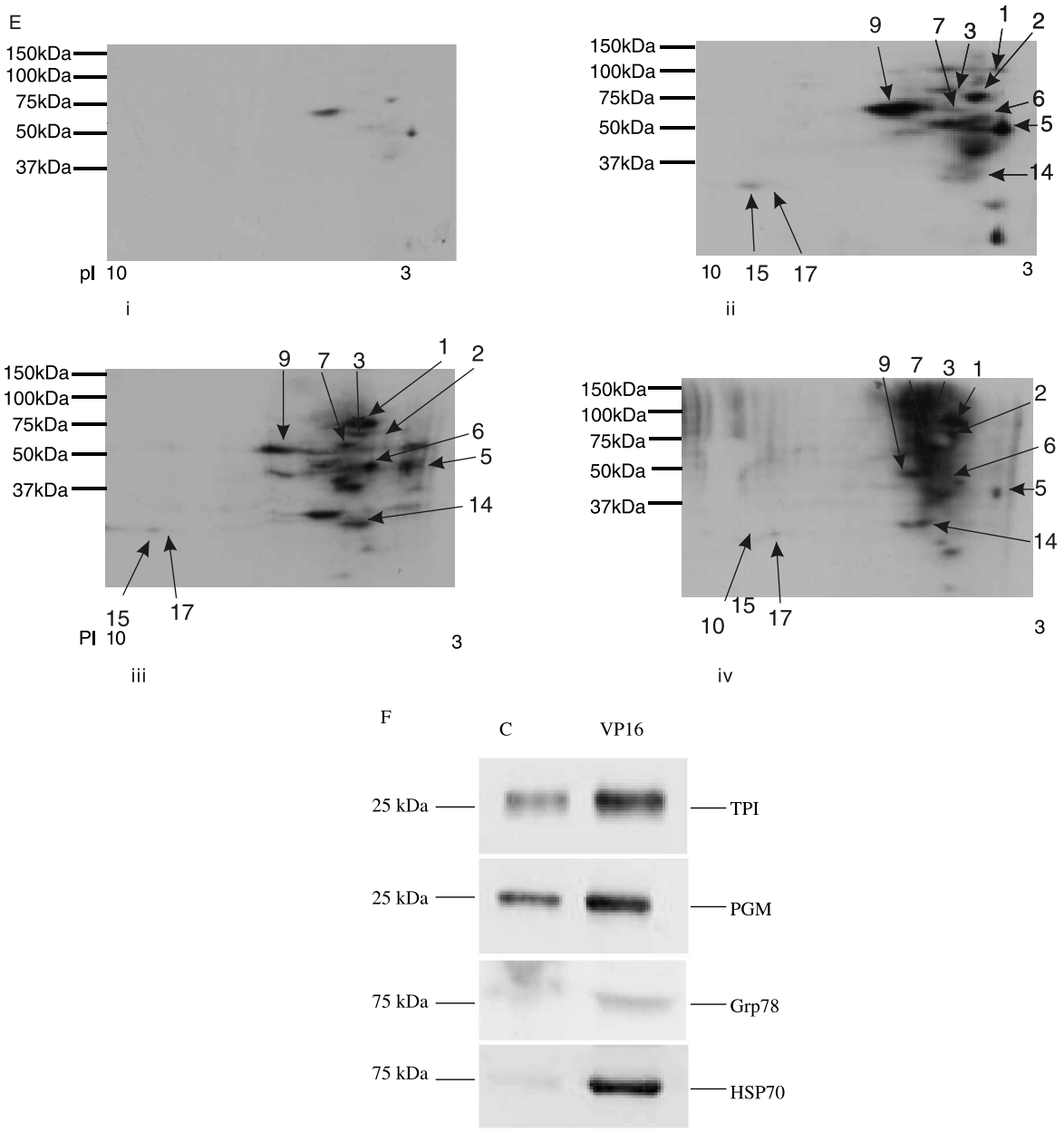

Figure 2. Induction of ROS and protein oxidation in response to VP16, Mtx and Doxo. A. Flow cytometric analysis shows that treatment with 5 μg/ml VP16, 10 μg/ml Mtx or 10 μg/ml Doxo result in an increase in cellular ROS within 15 min as detected by the fluorescent probe H_2DCFHDA. (i) single line-untreated HL60 cells, bold line-VP16 treated cells; (ii) single line-untreated HL60 cells, bold line-Mtx treated cells; and (iii) single line-untreated HL60 cells, bold line-Doxo treated cells. B. Histogram showing average mean H_2DCFHDA fluorescence after 15 min of drug treatment. C. Global protein carbonylation was determined spectrophotometrically using DNPH incorporation after 1 h of drug treatment with 5 μg/ml VP16, 10 μg/ml Mtx or 10 μg/ml Doxo ± the addition of 0.5 mM *N*-acetylcysteine for 15 min prior to cytotoxic drug addition. D. HL60 cells were treated with 0.5 mM *N*-acetylcysteine for 15 min prior to the addition of 5 μg/ml VP16. Cell death was determined after 4 h using propidium iodide exclusion assay and flow cytometry. E. 2D Oxyblots. Protein from control and drug treated cells underwent isoelectric focussing followed by DNPH treatment. Blots were probed with a DNP specific antibody to detect carbonylated proteins. (i) Untreated cells; (ii) 5 μg/ml VP16 treatment for 1 h; (iii) 10 μg/ml Mtx treatment for 1 h; and (iv) 10 μg/ml Doxo treatment for 1 h. Identified protein spots are annotated and correspond to those listed in Table I. F. Confirmation of carbonylated proteins through co-immunoprecipitation studies. Immunoprecipitations of triose phosphate isomerase, Phosphoglycerate mutase, Grp78 and HSP 70, from untreated (c) and VP16 treated cells. IPs were treated with DNPH, resolved by SDS-PAGE and probed with an anti-DNP antibody. In all cases, a protein band was detected at the correct size, indicating carbonylation, which increased upon cytotoxic drug treatment.

confirmed the identity of a number of carbonylated proteins through a reverse immunoprecipitation approach (Figure 2F). TPI, PGM, Grp78 and HSP 70 were immunoprecipitated from untreated and VP16 treated cells, derivitized with DNPH. Western blotting revealed the presence of a DNP immunoreactive protein (carbonylated protein) at the correct size for the specific proteins, confirming their immunoprecipitation. In all cases, carbonylation increased with drug treatment over that of untreated controls.

Table II. Protein modifications and during cytotoxic treatment of HL60 cells.

Spot no.	Protein name	Effect of VP16 treatment	Function	Location
1	90 kDa Heat shock protein	Carbonylation	Chaperone protein	ER lumen
2	Grp78	Carbonylation	Chaperone protein	ER lumen
3	70 kDa Heat shock protein	Carbonylation	Chaperone protein	ER protein
4	ATP synthase	Modification not identified	Important in proton transport.	Membrane protein
5	Calreticulin	Carbonylation	Calcium binding protein	ER lumen
6	Tubulin	Carbonylation	Structural protein	Cytoplasm
7	Protein disulphide isomerase	Phosphorylation & carbonylation	Rearranges disulphide bonds, possible role oxidative stress.	ER Lumen
8	Glycogen phosphorylase	Modification not identified	Role in carbohydrate metabolism	Cytoplasm
9	Alpha enolase	Carbonylation	Glycolytic enzyme	Cytoplasm
10	40s Ribosomal protein	Phosphorylation	Member of ribosomal protein family, associated with drug resistance	Cytoplasm
11	Inorganic pyrophosphatase	Modification not identified	Pyrophosphatase activity	Cytoplasm
12	Fructose bisphosphate aldolase	Carbonylation	Glycolytic enzyme	Cytoplasm
13	Tropomyosin	Modification not identified	Role in maintaining actin cytoskeleton	Cytoplasm
14	Endoplamic reticulum protein ERP29	Carbonylation	Role in processing secretory proteins,	ER lumen
15	Phosphoglycerate mutase	Carbonylation	Glycolytic emzyme	Cytoplasm
16 & 17	Triose phosphate isomerase	Carbonylation	Important in glycoclysis as well as other metabolic pathways.	Cytoplasm
18	Prohibitin	Modification not identified	Regulates proliferation by inhibiting DNA synthesis.	Cytoplasm
19	RHO GDP dissociation inhibitor 2	Modification not identified	Regulates RHO proteins by inhibitng GDP dissociation.	Cytoplasm
20	Glutathione S-transferase	Modification not identified	Redox regulation	Cytoplasm

Protein spots are listed along with their identity, modification-if identified, function and localisation.

Our data shows that drug induced ROS, resulting in protein oxidation is not restricted to VP16 treatment of HL60 cells, but also occurs with Mtx and Doxo treatment and that carbonylated proteins do not vary between drug treatments. It is possible that the reason we have identified similar proteins undergoing carbonylation in all drug treatments is that these are relatively abundant proteins. Such proteins may be more likely to undergo carbonylation and are more readily detected using our immunoprecipitation approach [20].

ER protein oxidation

Protein oxidation causes protein misfolding. Accumulation of misfolded protein within the ER leads to induction of ER stress and the unfolded protein response (UPR) [32]. In order to study whether cytotoxic drug treatment of HL60 cells had induced ER stress, we looked for two markers, the induction of eIF-2α phosphorylation and release of ER calcium. Western blot analysis showed increased levels of eIF-2α after treatment with all three drugs for 1 h (Figure 3A).

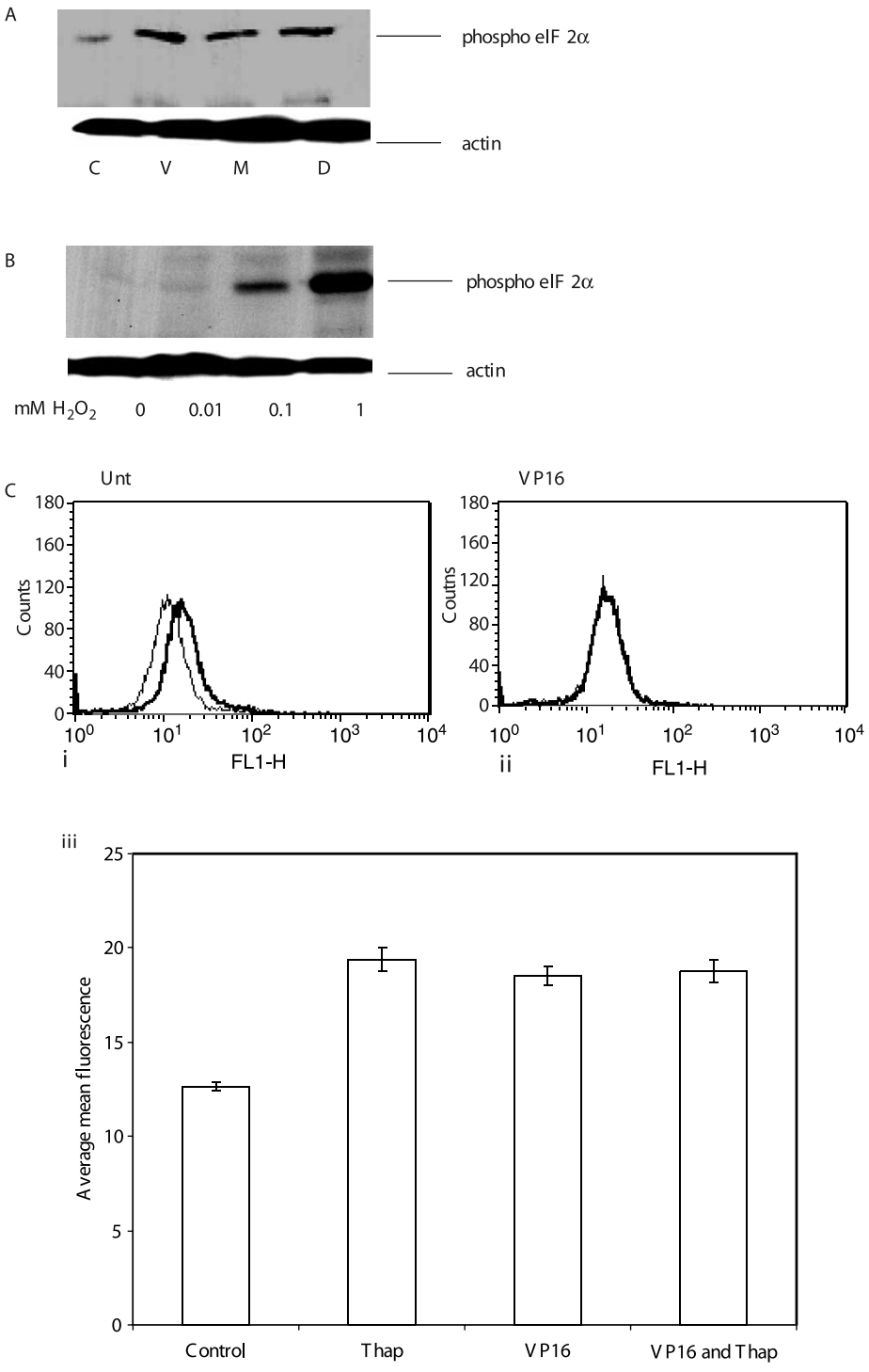

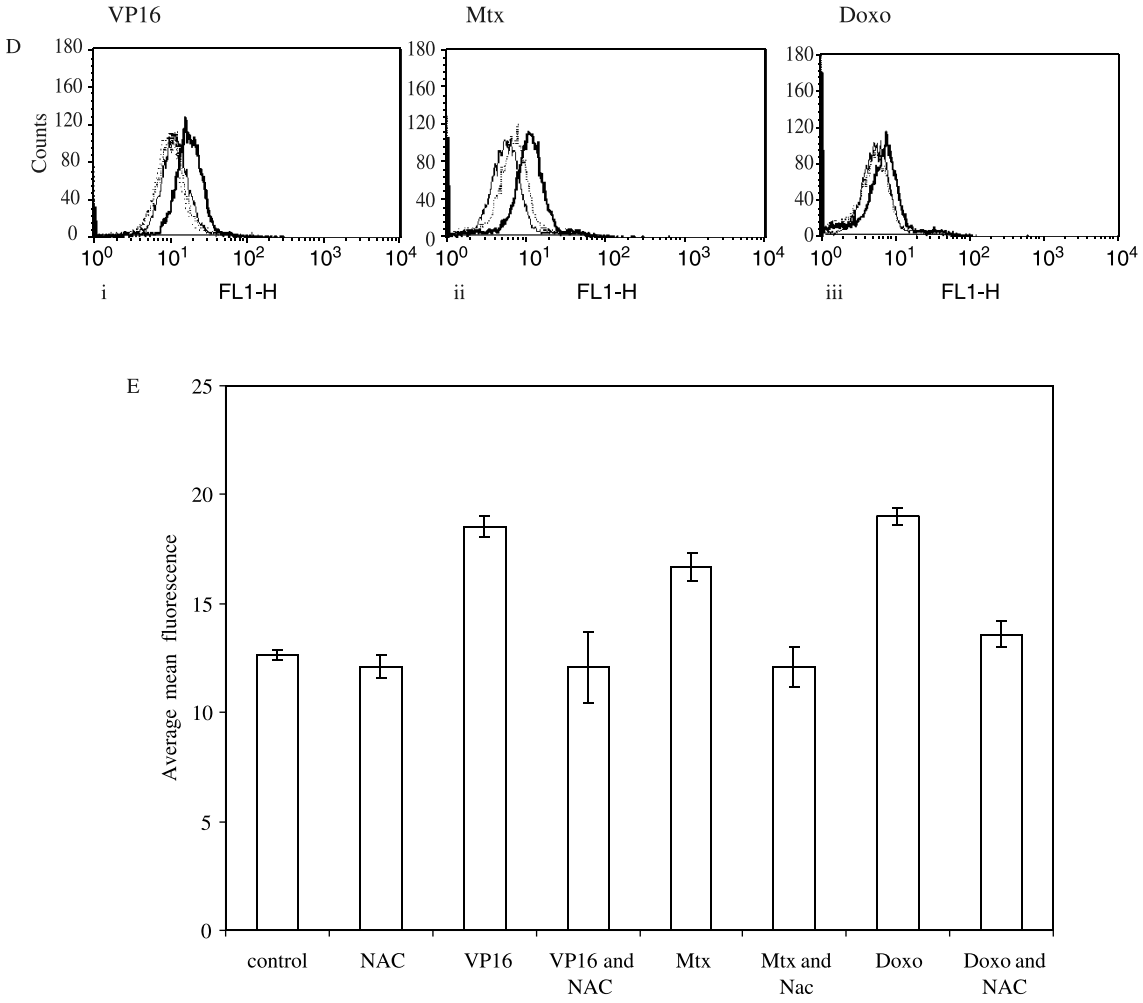

Figure 3. Protein oxidation induced ER stress. A. Western blot analysis using a phospho-eIF-2α specific antibody shows phosphorylation in untreated HL60 cells (C) and cells treated for 30 min with 5 μg/ml VP16 (V), 10 μg/ml Mtx or 10 μg/ml Doxo. Actin is used to show equal loading. B. eIF-2α phosphorylation is induced in response to ROS. Western blot analysis with a specific phospho- eIF-2α antibody shows a concentration dependant increase in eIF-2α phosphorylation in response to treatment with H_2O_2. Actin is shown to demonstrate equal loading. C. Cytosolic calcium was detected using flow cytometry and the Ca^{2+} specific probe Ca green. Ca green fluorescence from untreated HL60 cells and cells treated with 5 μg/ml VP16 for 1 h was recorded before and immediately after treatment with 5 μg/ml thapsigargin. (i) Single line-control cells, bold line-control cells following thapsigargin treatment; (ii) single line-VP16 treated cells, bold line-VP16 treated cells after thapsigargin treatment; and (iii) histogram showing average mean Ca green fluorescence in control and cells treated with 5 μg/ml VP16 for 1 h, before and after treatment with 5 μg/ml thapsigargin. D. Cytosolic calcium was detected using flow cytometry and the Ca^{2+} specific probe Ca green. An increase in intracellular calcium was detected after 1 h of treatment with 5 μg/ml VP16, 10 μg/ml Mtx, or 10 μg/ml Doxo and could be prevented by pre-treatment with 0.5 mM NAC. (i) Single line-control cells, bold line-cells treated with 5 μg/ml VP16, dashed line-cells treated with both 0.5 mM NAC and 5 μg/ml VP16; (ii) single line-control cells, bold line-cells treated with 10 μg/ml Mtx, dashed line-cells treated with both 0.5 mM NAC and 10 μg/ml Mtx; and (iii) Single line-control cells, bold line-cells treated with 10 μg/ml Doxo, dashed line-cells treated with both 0.5 mM NAC and 10 μg/ml Doxo. E. Histogram showing average mean Ca green fluorescence in drug and NAC pre-treated cells after 1 h of treatment.

Induction of eIF2-α phosphorylation could also be increased by treatment of HL60 cells with hydrogen peroxide (H_2O_2) (Figure 3B), implicating a role for ROS. This data supports our theory that drug induced protein carbonylation results in increased levels of oxidised proteins within the ER leading to increased ER stress. As ER stress can result in the release of Ca^{2+} from the ER into the cytosol, we looked for evidence of this in drug treated HL60 cells. We found that Ca^{2+} release does not occur immediately upon drug treatment, but is apparent after 1 h (data not shown). In order to confirm that the increase in cytosolic Ca^{2+} seen was due to ER Ca^{2+} release, we used thapsigargin. Thapsigargin stimulates ER Ca^{2+} release. In our system, thapsigargin treatment resulted in further increase in cytosolic Ca^{2+} in untreated cells in contrast to in drug treated cells where thapsigargin did not cause a further increase in cytosolic Ca^{2+} levels (indicating that the ER has already released its Ca^{2+}) (Figure 3C). All three drugs caused an increase in cytosolic Ca^{2+}, as determined by Ca green fluorescence, after 1 h and this increase could be blocked by pre-incubation with the

anti-oxidant NAC (Figure 3D and E) indicating a role for ROS in drug mediated ER Ca^{2+} release. These data support our theory that accumulation of misfolded, oxidised proteins within the ER results in induction of the UPR and Ca^{2+} release. This can result in the induction of apoptosis and may be key mechanisms of action for these drugs.

Discussion

Using a proteomic approach, we have identified a number of proteins which undergo changes in HL60 cells treated with VP16, Mtx and Doxo. These changes occurred at early time points, all were detectable after 1 h of treatment and were not dependent on new protein synthesis or degradation. During this study, we have looked for a number of PTM, which result in the changes in protein patterns seen. We found no evidence of drug induced protein ADP ribosylation or s-nitrosylation and few proteins which underwent cytotoxic drug dependant phosphorylation.

However our proteomic approach identified several proteins undergoing oxidation during VP16, Mtx and Doxo treatment due to increased levels of cellular ROS. ROS are constantly being generated within the cell by metabolic processes. ROS can be also be generated within the cell as a response to cell stress and may act as secondary messengers [33] to stimulate cell death from apoptosis or necrosis [6,34]. ROS include free radicals such as the superoxide anion ($O_2^{-\cdot}$), hydoxyl radicals ($^{\cdot}OH$) and H_2O_2. ROS can react with and so damage, proteins, as well as lipids and carbohydrates. Treatment of cells with many cytotoxic drugs has been shown to result in the production of ROS, although their importance in drug induced cell death is controversial. For example, VP16 has been reported in the literature to induced cell death through pathways independent of topoisomerase II inhibition but dependant of ROS production, although in other systems, antioxidant treatments do not inhibit VP16 induced cell death [5,6]. It has been suggested that ROS release in response to Doxo is important in cardiotoxicity and that, ROS release may be differential between tumour and normal cells [8]. In the case of Doxo, the mechanism of ROS generation has been described. A quinone group undergoes reduction to the semi-quinone free radical through the action of NADH dehydrogenase. In the presence of oxygen, this will form superoxide, which in turn is converted to H_2O_2 by the action of superoxide dismutase [35]. ROS generation by other cytotoxic drug treatments may results from direct action of enzymes on drugs to form reactive metabolites, or indirect actions of the drug resulting in an induction of ROS through activation of cell stress pathways. It is likely that the generation of ROS by cytotoxic drug treatment of cells results in non-enzymatic protein modifications that may play an important role in the early stages of apoptosis.

ROS can cause a number of non-enzymatic modifications of proteins, including carbonylation, *o*-tyrosine, chloro-, nitrotyrosine and dityrosine. Protein carbonylation is often used as a marker for oxidative stress [36]. Protein carbonylation can occur through direct oxidation of amino acid side chains with ROS including H_2O_2 and HOCl through Fenton chemistry [37,38]. Alternatively, amino acids can react with products of lipid peroxidation, such as 4-hydoxyl-2-nonenal by Michael addition reactions [39–41]. Carbonylation of proteins can also occur through reaction with reducing sugars or their oxidation products (glycation) [38–40]. As carbonylation involves the addition of a relatively large and reactive group onto the peptide backbone of a protein, it can have a variety of effects on the proteins properties, including covalent intermolecular cross-linking [38,42] but most significantly, carbonylation of a protein can also reduce its activity [22]. For example, glutamine synthase exposed to metal catalysed oxidation has reduced enzyme activity [4]. Consequently, cells that have large numbers of protein carbonyls may be expected to have impaired function.

Protein oxidation has been shown to be important in the induction of cell death in a variety of systems, however, it is only with recent technologies, such as proteomics, that it has been possible to discover which proteins undergo oxidation and so to understand the role that protein oxidation plays in cell death. It is clear from a number of studies that some key proteins are particularly susceptible to protein carbonylation. Across both bacterial, yeast and mammalian systems, glycolytic and ER proteins, especially chaperone proteins, have been shown to undergo carbonylation in response to ROS, typically during ageing [19,20,43–47]. The oxidation of glycolytic proteins may result in a reduction of glycolysis; this in itself may result in a decrease in ROS production due to decreased mitochondrial activity. A reduction in glycolytic activity may also result in an increase in activity of the pentose phosphate pathways, resulting in an increase in NADPH levels [46], a key component of cellular antioxidants. However, we have reported previously that in HL60 cells, inhibition of glycolysis did not result in an increase in the pentose phosphate pathway [19].

The observation that ER proteins are readily carbonylated is interesting given the importance of the ER in the induction of apoptosis. The ER regulates both protein folding and storage of Ca^{2+}, alterations in both of these can lead to apoptosis. The ER is a site of ROS production and in contrast to the mitochondria has few anti-oxidant defences. It also has a highly redox environment and iron is present, both of which are important for protein carbonylation. As such, the ER is likely to be especially susceptible to protein

carbonylation and other oxidative stress mediated protein modifications. Indeed, Rabek et al. recently demonstrated carbonylation of ER proteins in aged mouse liver [48]. Grp78 has been shown to be play a role in resistance to induction of cell death by topoisomerase II inhibitors such as VP16 [49], so its inactivation by carbonylation may be critical for the induction of cell death in our system. PDI, GRP78 and HSP 70 and 90 act as chaperone proteins, important in detecting the presence of misfolded proteins in the ER. Carbonylation of these proteins is likely to inhibit the function of these proteins, increasing the amount of misfolded proteins within the ER and through this, induce the UPR, as we have demonstrated through the induction of eIF-2α phosphorylation.

Activation of the UPR by cell stress results in transcriptional induction of ER chaperones to increase the protein folding capacity of the ER, but can also result in the induction of apoptosis [32]. It is possible that induction of the UPR by the presence of misfolded and oxidised proteins within the ER can induce ER Ca^{2+} release, however, it is also possible that ER Ca^{2+} release can affect protein folding and hence induce the UPR. Given the timing of the events in our cell system; induction of the UPR is detected with 1 h of drug treatment, as is calcium release, it is not clear which occurs first. However, as there is no rapid calcium release in response to drug treatments, we suggest that the most likely scenario is that ROS release results in ER stress and activation of the UPR and that this is upstream of ER calcium release. ER Ca^{2+} release is mediated by, among others, the Bcl-2 family of apoptotic regulators. Overexpression of Bax or Bak leads to ER Ca^{2+} release, Ca^{2+} influx into the mitochondria, and cytochrome c release, causing further ER Ca^{2+} release [50,51]. In mice, caspase 12 is activated by ER stress and mediates further activation of the caspase cascade. No human homologue for caspase 12 has been identified as yet, although, there is some data suggesting that caspase 4 performs a similar role in humans[52].

This study demonstrates a role for ROS mediated signalling events in response to cytotoxic drug treatment. Although it is possible that the mechanism of action of any particular drug vary between cell types, our work clearly implicates ROS as an early mediator of cytotoxic drug induced apoptosis. In particular, this work suggests a role for oxidised proteins in induction of ER stress, through which apoptosis may become inevitable.

Acknowledgements

This work is funded by Cancer Research Ireland. The authors would like to thank Dr F. Hickey and Dr S. Clerkin for useful discussion and reading of the manuscript.

References

[1] Fisher D. Apoptosis in cancer therapy: Crossing the threshold. Cell 1994;78:539–542.
[2] Herr I, Debatin KM. Cellular stress response and apoptosis in cancer therapy. Blood 2001;98(9):2603–2614.
[3] Armstrong SC. Anti-oxidants and apoptosis: Attenuation of doxorubicin induced cardiomyopathy by carvedilol. J Mol Cell Cardiol 2004;37(4):817–821.
[4] Ma YS, Chao CC, Stadtman ER. Oxidative modification of glutamine synthetase by 2,2′-azobis(2-amidinopropane) dihydrochloride. Arch Biochem Biophys 1999;363(1):129–134.
[5] Troyano A, Fernandez C, Sancho P, de Plas E, Aller P. Effect of glutathione depeation on antitumour drug toxicity (apoptosis and necrosis) in U-937 human promonocytic cells—the role of intracellular oxidation. J Biol Chem 2001;276(50):47107–47115.
[6] Gorman A, McGowan A, Cotter TG. Role of peroxide and superoxide anion during tumour cell apoptosis. FEBS Lett 1997;404(1):27–33.
[7] Mizutani H, Tada-Oikawa S, Hiraku Y, Kojima M, Kawanishi S. Mechanism of apoptosis induced by doxorubicin through the generation of hydrogen peroxide. Life Sci 2005;76(13):1439–1453.
[8] Wang SW, Konorev EA, Kotamraju S, Joseph J, Kalivendi S, Kalyanaraman B. Doxorubicin induces apoptosis in normal and tumor cells via distinctly different mechanisms—intermediacy of H_2O_2- and p53-dependent pathways. J Biol Chem 2004;279(24):25535–25543.
[9] Tsang WP, Chau SPY, Kong SK, Fung KP, Kwok TT. Reactive oxygen species mediate doxorubicin induced p53-independent apoptosis. Life Sci 2003;73(16):2047–2058.
[10] Kang YJ, Zhou ZX, Wang GW, Buridi A, Klein JB. Suppression by metallothionein of doxorubicin-induced cardiomyocyte apoptosis through inhibition of p38 mitogen-activated protein kinases. J Biol Chem 2000;275(18): 13690–13698.
[11] Stadheim TA, Kucera GL. c-Jun *N*-terminal kinase/stress-activated protein kinase (JNK/SAPK) is required for mitoxantrone- and anisomycin-induced apoptosis in HL-60 cells. Leuk Res 2002;26(1):55–65.
[12] Wang L, Chen L, Benincosa J, Fortney J, Gibson LF. VEGF-induced phosphorylation of Bcl-2 influences B lineage leukemic cell response to apoptotic stimuli. Leukemia 2005;19(3):344–353.
[13] Colussi C, Albertini MC, Coppola S, Rovidati S, Galli F, Ghibelli L. H_2O_2-induced block of glycolysis as an active ADP-ribosylation reaction protecting cells from apoptosis. FASEB J 2000;14(14):2266–2276.
[14] Scovassi AI, Poirier GG. Poly(ADP-ribosylation) and apoptosis. Mol Cell Biochem 1999;199(1–2):125–137.
[15] Ghibelli L, Nosseri C, Coppola S, Maresca V, Dini L. The increase in H_2O_2-induced apoptosis by ADP-ribosylation inhibitors is related to cell blebbing. Exp Cell Res 1995;221(2):470–477.
[16] Monteiro H, Tsujita M, Arai R, Stern A. Ras nitrosylation and protein phosphorylation in nitric oxide-induced apoptosis. Free Radic Biol Med 2003;35:S70–S71.
[17] Tenneti L, Demilia DM, Lipton SA. Suppression of neuronal apoptosis by S-nitrosylation of caspases. Neurosci Lett 1997;236(3):139–142.
[18] Melino G, Bernassola F, Knight RA, Corasaniti MT, Nistico G, FinazziAgro A. S-nitrosylation regulates apoptosis. Nature 1997;388(6641):432–433.
[19] England K, O'Driscoll C, Cotter TG. Carbonylation of glycolytic proteins is a key response to drug induced oxidative stress and apoptosis. Cell Death Differ 2004;11:252–260.

[20] England K, Cotter T. Identification of carbonylated proteins by MALDI-TOF mass spectroscopy reveals susceptibility of ER. Biochem Biophys Res Commun 2004;320(1):123–130.
[21] Melino G, Catani MV, Corazzari M, Guerrieri P, Bernassola F. Nitric oxide can inhibit apoptosis or switch it into necrosis. Cell Mol Life Sci 2000;57(4):612–622.
[22] Fucci L, Oliver CN, Coon MJ, Stadtman ER. Inactivation of key metabolic enzymes by mixed-function oxidation reactions: Possible implication in protein turnover and ageing. Proc Natl Acad Sci USA 1983;80:1521–1525.
[23] Levine RL, Garland D, Oliver CN, Amici A, Climent I, Lenz A-G, Ahn BW, Shaltiel S, Stadtman ER. Determination of carbonyl content in oxidatively modified proteins. Methods Enzymol 1990;186:464–478.
[24] Ellgaard L, Ruddock LW. The human protein disulphide isomerase family: Substrate interactions and functional properties. EMBO Rep 2005;6(1):28–32.
[25] Frand AR, Cuozzo JW, Kaiser CA. Pathways for protein disulphide bond formation. Trends Cell Biol 2000;10(5): 203–210.
[26] Ferrari DM, Soling HD. The protein disulphide-isomerase family: Unravelling a string of folds. Biochem J 1999;339:1–10.
[27] Tanaka Y, Gavrielides MV, Mitsuuchi Y, Fujii T, Kazanietz MG. Protein kinase C promotes apoptosis in LNCaP prostate cancer cells through activation of p38 MAPK and inhibition of the Akt survival pathway. J Biol Chem 2003;278(36): 33753–33762.
[28] Tamagno E, Robino G, Obbili A, Bardini P, Aragno M, Parola M, Danni O. H_2O_2 and 4-hydroxynonenal mediate amyloid beta-induced neuronal apoptosis by activating JNKs and p38(MAPK). Exp Neurol 2003;180(2):144–155.
[29] Kondoh M, Tasaki E, Araragi S, Takiguchi M, Higashimoto M, Watanabe Y, Sato M. Requirement of caspase and p38(MAPK) activation in zinc-induced apoptosis in human leukemia HL-60 cells. Eur J Biochem 2002;269(24): 6204–6211.
[30] Alvarado-Kristensson M, Andersson T. Protein phosphatase 2A regulates apoptosis in neutrophils by dephosphorylating both p38 MAPK and its substrate caspase 3. J Biol Chem 2005;280(7):6238–6244.
[31] Perfettini JL, Castedo M, Nardacci R, Ciccosanti F, Boya P, Roumier B, Larochette N, Piacentini M, Kroemer G. Essential role of p53 phosphorylation by p38 MAPK in apoptosis induction by the HIV-1 envelope. J Exp Med 2005;201(2): 279–289.
[32] Rao RV, Ellerby HM, Bredesen DE. Coupling endoplasmic reticulum stress to the cell death program. Cell Death Differ 2004;11(4):372–380.
[33] Carmody RJ, Cotter TG. Signalling apoptosis:a radical approach. Redox Rep 2001;6(2):77–90.
[34] McGowan AJ, Fernandes RS, Samali A, Cotter TG. Anti-oxidants and apoptosis. Biochem Soc Trans 1996;24: 299–303.
[35] Lown JW, Chen HH, Plambeck JA, Acton EM. Further studies on the generation of reactive oxygen species from activated anthracyclines and the relationship to cytotoxic action and cardiotoxic effects. Biochem Pharmacol 1982;31:575–581.
[36] Chevion M, Berenshtein E, Stadtman ER. Human studies related to protein oxidation: Protein carbonyl content as a marker of damage. Free Radic Res 2000;33:S99–S108.
[37] Wondrak GT, Cervantes-Laurean D, Jacobson EL, Jacobson MK. Histone carbonylation *in vivo* and *in vitro*. Biochem J 2000;351:769–777.
[38] Berlett BS, Stadtman ER. Protein oxidation in aging, disease, and oxidative stress. J Biol Chem 1997;272(33): 20313–20316.
[39] Stadtman ER. Role of oxidized amino-acids in protein breakdown and stability, in redox-active amino acids in biology Redox-active amino-acids in biology. 1995. p 379–393.
[40] Dean RT, Fu SL, Stocker R, Davies MJ. Biochemistry and pathology of radical-mediated protein oxidation. Biochem J 1997;324:1–18.
[41] Stadtman ER, Berlett BS. Reactive oxygen mediated protein oxidation in aging and disease. In: Colton C, Gilbert DJ, editors. Reactive oxygen species in biological systems. New York: Kluwer Academic/Plenum Publishers; 1999. p 657–675.
[42] Burcham PC, Kuhan YT. Diminished susceptibility to proteolysis after protein modification by the lipid peroxidation product malondialdehyde: Inhibitory role for crosslinked and noncrosslinked adducted proteins. Arch Biochem Biophys 1997;340(2):331–337.
[43] Cabiscol E, Belli G, Tamarit J, Echave P, Herrero E, Ros J. Mitochondrial Hsp60, resistance to oxidative stress, and the labile iron pool are closely connected in *Saccharomyces cerevisiae*. J Biol Chem 2002;277(46):44531–44538.
[44] Tamarit J, Cabiscol E, Ros J. Identification of the major oxidatively damaged proteins in *Escherichia coli* cells exposed to oxidative stress. J Biol Chem 1998;273(5):3027–3032.
[45] Cabiscol E, Piulats E, Echave P, Herrero E, Ros J. Oxidative stress promotes specific protein damage in *Saccharomyces cerevisiae*. J Biol Chem 2000;275(35):27393–27398.
[46] Godon C, Lagniel G, Lee J, Buhler JM, Kieffer S, Perrot M, Boucherie H, Toledano MB, Labarre J. The H_2O_2 stimulon in *Saccharomyces cerevisiae*. J Biol Chem 1998;273(35): 22480–22489.
[47] Reverter-Branchat G, Cabiscol E, Tamarit J, Ros J. Oxidative damage to specific proteins in replicative and chronological-aged *Saccharomyces cerevisiae*: Common targets and prevention by calorie restriction. J Biol Chem 2004;279(30): 31983–31989.
[48] Rabek JP, Boylston WH, Papaconstantinou J. Carbonylation of ER chaperone proteins in aged mouse liver. Biochem Biophys Res Commun 2003;305(3):566–572.
[49] Reddy RK, Mao C, Baumeister P, Austin RC, Kaufman RJ, Lee AS. Endoplasmic reticulum chaperone protein GRP78 protects cells from apoptosis induced by topoisomerase inhibitors: Role of ATP binding site in suppression of caspase-7 activation. J Biol Chem 2003;278(23): 20915–20924.
[50] Nutt L, Chandra J, Pataer A, Fang B, Roth J, Swisher S, O'Neill R, McConkey D. Bax mediated Ca^{2+} mobilization promotes cytochrome C release during apoptosis. J Biol Chem 2002;277:20301–20308.
[51] Nutt L, Pataer A, Pahler J, Fang B, Roth J, McConkey D, Swisher S. Bax and Bak promote apoptosis by modulating endoplasmic reticular and mitochondrial Ca^{2+} stores. J Biol Chem 2002;277:9219–9225.
[52] Ma YJ, Hendershot LM. The role of the unfolded protein response in tumour development: Friend or foe? Nat Rev Cancer 2004;4(12):966–977.